Glycoconj J (2010) 27:625–633
DOI 10.1007/s10719-010-9306-1

RGD-xyloside conjugates prime glycosaminoglycans

Vy M. Tran · Xylophone V. Victor · James W. Yockman · Balagurunathan Kuberan

Received: 25 May 2010 / Revised: 28 July 2010 / Accepted: 5 August 2010 / Published online: 18 August 2010

Abstract Glycosaminoglycans (GAG) play decisive roles in various cardio-vascular & cancer-associated processes. Changes in the expression of GAG fine structures, attributed to deregulation of their biosynthetic and catabolic enzymes, are hallmarks of vascular dysfunction and tumor progression. The wide spread role of GAG chains in blood clotting, wound healing and tumor biology has led to the development of modified GAG chains, GAG binding peptides and GAG based enzyme inhibitors as therapeutic agents. Xylosides, carrying hydrophobic aglycone, are known to induce GAG biosynthesis in various systems. Given the important roles of GAG chains in vascular and tumor biology, we envision that RGD-conjugated xylosides could be targeted to activated endothelial and cancer cells, which are known to express $\alpha_v\beta_3$ integrin, and thereby modulate the pathological processes. To accomplish this vision, xylose residue was conjugated to linear and cyclic RGD containing peptides using click chemistry. Our results demonstrate that RGD-conjugated xylosides are able to prime GAG chains in various cell types, and future studies are aimed toward evaluating potential utility of such xylosides in treating myocardial infarction as well as cancer-associated thrombotic complications.

Keywords Proteoglycans · Glycosaminoglycans · Xylosides · RGD targeting · Biosynthesis · Heparan sulfate · Tumor · Cardiovascular · Chondroitin sulfate

Abbreviations

GAG	chains-Glycosaminoglycans
RGD	Arginine-Glycine-Aspartate
HS	Heparan Sulfate
CS	Chondroitin Sulfate
DS	Dermatan Sulfate
BLMVEC	Bovine Lung Endothelial vascular Cell
4T1	Mouse Breast Cancer Cell

Introduction

Proteoglycans (PG) consist of a core protein and one or more GAG chains. There are four major classes of sulfated GAG chains: heparan sulfate (HS), chondroitin sulfate (CS), dermatan sulfate (DS) and keratan sulfate. GAG side chains of PGs play an important role in various cardiovascular functions including haemostasis and thrombosis [1]. HS chains that contain a specific pentasaccharide sequence function as an endogenous anticoagulant through inhibition of factor Xa by activating anti-thrombin III (ATIII) [2–4]. One of the main causes of myocardial infarction (MI), a devastating disease that kills several million people world-

V. M. Tran · B. Kuberan
Department of Bioengineering,
University of Utah,
Salt Lake City, UT 84112, USA

X. V. Victor · B. Kuberan (✉)
Department of Medicinal Chemistry,
University of Utah,
Skaggs Hall Rm#307, 30 South 2000 East,
Salt Lake City, UT 84112, USA
e-mail: KUBY@pharm.utah.edu

J. W. Yockman
Department of Pharmaceutics & Pharmaceutical Chemistry,
University of Utah,
Salt Lake City, UT 84112, USA

B. Kuberan
Graduate Program in Neuroscience,
University of Utah,
Salt Lake City, UT 84112, USA

wide annually, is the formation of thrombi inside the coronary artery through platelet activation/aggregation. GAG side chains also play a major role in various cancer processes. Dramatic changes in the expression of biosynthetic and catabolic enzymes are attributed to alterations in GAG fine structures, which are suggested to affect tumor cell growth, invasion and metastasis [5, 6]. For example, heparanase, a β-endoglucuronidase which is over expressed in a variety of malignant tumors, cleaves HS chains into smaller biologically active oligosaccharides that promote cancer growth, angiogenesis, tumor-cell invasion and migration [7–9]. Melanoma associated CS and DS chains have been shown to stimulate tumor cell proliferation [10], while these GAG chains have been shown to surprisingly suppress angiogenesis [11].

Heparin, structurally similar to HS, has been in use as a major anticoagulant for seven decades because of its abundance, cost and potency. It is used as a blood thinner in surgical procedures and in tackling thrombotic complications associated with various cardiovascular and cerebrovascular dysfunctions. Heparin is also known to affect tumor biology in a variety of ways [11–13]. It decreases thrombin generation and fibrin formation, inhibits heparanase, modulates P-selectin-vascular wall interactions and adhesion. A chemically modified non-anticoagulant heparin-like molecule is shown to reduce metastasis by more than 50% [11]. In various clinical trials, low molecular weight heparin is shown to increase survival rate among patients with advanced malignancy.

Several animal derived GAGs and their derivatives have been in use as therapeutics to tackle thrombosis, MI and cancer. However, direct administration of these GAG chains faces the problem of molecular heterogeneity, possible contamination with pathogens or intentional chemical adulteration as evidenced in the latest tragic episode of heparin contamination [14, 15]. Furthermore, it is administered intravenously, which makes it is less attractive for those who require prolonged prophylactic treatment. An alternative approach would be the use of xylosides to induce endogenous GAG chain biosynthesis without a core protein at specific sites. Xylosides containing a hydrophobic aglycone can compete with endogenous core protein acceptor sites for assembly of GAG chains in the Golgi apparatus [16–22]. The hydrophobic aglycone helps xylosides pass through the membrane and hence increases priming activity/production of GAG chains and its oral bioavailability. Interestingly, the composition of primed GAG chains depends on the structure of the aglycone moiety [23–25].

Arginine-glycine-aspartate (RGD) selectively binds to $\alpha_v\beta_3$ integrin, which is abundantly expressed on the surface of many tumor cell types and activated endothelial cells surrounding cancer and myocardial infarction. Linear and cyclic peptide sequences containing RGD motifs have been employed as targeting vectors for selective delivery of therapeutic and diagnostic agents by conjugating them to RGD sequences [26–30]. Moreover, RGD derivatives are also shown to interact selectively with the GPIIb/IIIa receptor and therefore inhibit platelet aggregation [31]. Therefore, RGD-conjugated xylosides are predicted to have a dual use as anticoagulants as well as anti-platelet agents in tackling thrombotic complications associated with MI, cancer and other disease conditions. Here, we describe the synthesis of RGD—conjugated xylosides using click-chemistry and report on their GAG priming activity in a variety of cellular systems.

Experimental section

Materials

Chinese hamster ovary (CHO) cell line, pgsA-745, which is defective in xylosyl transferase, was obtained from American Type Culture Collection. The cell culture reagents for CHO cell line were obtained from HyClone. Bovine lung microvascular endothelial cell (BLMVEC) and Mouse breast cancer cells (4T1) were gifts from Dr Randall Dull and Dr David Bull, University of Utah, respectively. The cell culture reagents for BLMVEC and 4T1 (MCDB-131 complete) were obtained from Vec Technologies. $Na_2{}^{35}SO_4$ was purchased from MP Biochemicals and Ultima-FloAP scintillation cocktail for flow scintillation analysis was obtained from PerkinElmer Life Sciences. All other chemicals and biochemicals were obtained from Sigma. Linear RGD peptide **4** was synthesized using peptide synthesizer available through core facilities at the University of Utah, and cyclic RGD peptide **7** was purchased from Peptides International Inc. The DEAE-Sepharose gel was purchased from Amersham Biosciences. The anion-exchange chromatography column TSK-GEL DEAE-3SW (7.4 mm×7.5 cm, 10 μm particle size) and the size exclusion chromatography columns G3000SWXL (7.8 mm×30 cm) were obtained from Tosoh Bioscience.

General synthetic procedures

Anhydrous solvents were purchased and used directly or dried over standard drying agents and freshly distilled prior to use. Reactions were monitored by TLC on silica gel 60 F_{254} with detection by Von's reagent. Intermediate compounds were purified by flash chromatography columns using silica gel 60 (230–400 mesh) and were run under pressure at 5–7 psi. Final products were purified by high performance liquid chromatography (HPLC) on reverse

phase C18 column (VYDAC 2.2 cm×25 cm) with solvent A (25 mM formic acid in water) and solvent B (95% acetonitrile) at a flow rate of 5 ml/min in a linear gradient over 120 min starting with 0% B. All synthetic compounds were characterized by mercury 400 MHz spectrometry. The compounds were also confirmed for their final structures using a Finnigan LCQ mass spectrometry in either positive or negative ion mode.

2,3,4-Tri-*O*-Acetyl-*β*-*D*-xylopyranosyl azide (**1**): Trimethylsilyl azide (1.5 mmol) and $SnCl_4$ (0.5 mmol) were added dropwise to a stirred solution of fully acetylated xylose derivative (1 mmol) in dry CH_2Cl_2, and stirring was continued at room temperature. The progress of the reaction was checked by TLC, and after the completion of the reaction, the reaction mixture was then evaporated under vacuum to give a residue that was further purified by low pressure flash silica column chromatography to yield the compound **1** [32].

N-(2,3,4-tri-*O*-acetyl-*β*-*D*-xylopyranosyl) chloroacetamide (**2**): 2,3,4-Tri-*O*-Acetyl-*β*-*D*-xylopyranosyl azide **1**) (1 mmol) was dissolved in dry CH_2Cl_2 (20 ml). The mixture was cooled at 0°C. Chloroacetic anhydride (1 mmol) was added to the solution, followed by triphenyl phosphine (1 mmol), and the reaction was continued overnight. After the reaction was complete, the solvent was removed using rotary evaporator under reduced pressure. The reaction mixture was extracted using ethyl acetate and water. The organic layer was washed with saturated brine solution and evaporated under vacuum to give a residue, which was purified by silica column chromatography to give the title compound **2** [33].

N-(2,3,4-tri-*O*-acetyl-*β*-xylopyranosyl) azidoacetamide (**3**): *N*-(2,3,4-tri-*O*-acetyl-*β*-*D*-xylopyranosyl) chloroacetamide **2**) (1 mmol) was taken in a 100 ml RB flask and dry DMF (20 ml) was added, followed by the addition of sodium azide (2 mmol). The reaction mixture was heated to 90°C under stirring. Progress of the reaction was monitored by TLC using ethyl acetate and hexane (1:1) as the eluant. After the reaction was complete, the reaction mixture was cooled and diluted with ethyl acetate. The organic layer was washed with water, dried over sodium sulfate and concentrated to obtain a syrupy materials that was further purified by silica flash column chromatography to give the title compound **3** [34].

Propargylated cyclic RGD (**8**): Propiolic acid (10 mmol) was taken in a RB flask and dry DMF (20 ml) was added, followed by addition of hydroxybenzotriazole (5 mmol) and 1, 3-dispropylcarbodimide (5 mmol). The reaction mixture was stirred for 1 h before cyclic RGD (1 mmol) was added, and stirred for another hour. The reaction mixture was evaporated using a rotary evaporator under reduced pressure. The reaction mixture was purified by HPLC-reverse phase C18 column with solvent A (25 mM formic acid in water) and solvent B (95% acetonitrile) in a linear gradient starting with 0% B to give the pure compound 8.

Preparation of RGD-conjugated xylosides (**5**, **6** and **9**): To a solution of alkyne group containing linear or cyclic RGD derivative (1 mmol) and xylosyl azide derivative (1 mmol) in DMF (8 ml) / water (2.6 ml) mixture, sodium ascorbate (0.8 mmol) was added, followed by $Cu_2SO_4.5H_20$ (0.4 mmol) at room temperature and the mixture was stirred until the disappearance of the starting materials as indicated by TLC. At the end of the reaction, the reaction mixture was concentrated using the rotary evaporator under reduced pressure. The reaction mixture was purified by HPLC—reverse phase C18 column with solvent A (25 mM formic acid in water) and solvent B (95% acetonitrile) to give the final compounds, **5**, **6** & **9**. Compound **5**: ^{1}H NMR (CD_3OD): δ 8.07 (s, 1H), 5.97 (d, J=8.98 Hz, 1H), 5.55–5.44 (m, 2H), 5.20–5.14 (m, 1H), 4.58 (t, J=4.68 Hz, 1H), 4.46 (dd, J=15.62 Hz, 24.80 Hz, 2H), 4.41–4.36 (m, 1H), 4.22 (dd, J=5.47 Hz, 11.33 Hz, 1H), 4.02 (d, J=17.18 Hz, 1H), 3.74 (t, J=10.54 Hz, 1H), 3.72 (d, J=16.79 Hz, 1H), 3.26–3.20 (m, 1H), 3.12–3.05 (m, 1H), 2.92 (dd, J=4.3 Hz, 16.60 Hz, 1H), 2.53 (dd, J=5.08 Hz, 16.40 Hz, 1H), 2.04 (s, 3H), 2.01 (s, 3H), 2.00 (s, 3H), 1.82 (s, 3H), 1.70–1.64 (m, 2H); MS (ESI): calcd for $C_{28}H_{43}N_{10}O_{13}$ $[M+H]^+$ 727.2932; found 727.3333. Compound **6**: ^{1}H NMR (CD_3OD): δ 7.86 (s, 1H), 5.28 (t, J=9.37 Hz, 1H), 5.20 (d, J=8.98 Hz, 1H), 5.12 (d, J=1.95 Hz, 1H), 4.58–4.57 (m, 1H), 4.53 (s, 1H), 4.44 (s, 1H), 4.40–4.35 (m, 1H), 4.06–4.02 (m, 1H), 3.98 (s, 1H), 3.72 (d, J=16.79 Hz, 1H), 3.48 (t, J=11.13 Hz, 1H), 3.25–3.22 (m, 1H), 3.13–3.08 (m, 1H), 2.92 (dd, J=4.3 Hz, 16.4 Hz, 1H), 2.50 (dd, J=4.69 Hz, 16.60 Hz, 1H), 2.06–1.96 (m, 12 H), 1.68–1.63 (m, 2H) ; MS (ESI): calcd for $C_{30}H_{46}N_{11}O_{14}$ $[M+H]^+$ 784.3226; found 784.3400. Compound **9**: ^{1}H NMR (CD_3OD): δ 8.65 (s, 1H), 8.60 (s, 1H), 8.34 (s, 1H), 7.86 (d, J=6.64 Hz, 1H), 7.54 (t, J=7.81 Hz, 1H), 7.25–7.16 (m, 3H), 6.09 (d, J=8.98 Hz, 1H), 5.62–5.56 (m, 1H), 5.50 (t, J=8.98 Hz, 1H), 5.24–5.18 (m, 1H), 4.66 (t, J=5.08 Hz, 1H), 4.54 (t, J=6.64 Hz, 1H), 4.41 (t, J=6.64 Hz, 1H), 4.30–4.24

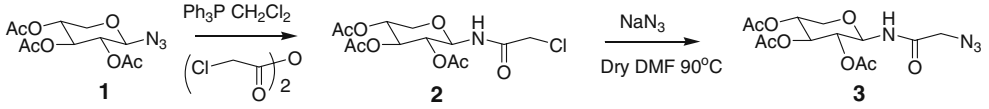

Scheme 1 Synthesis of *N*-(2,3,4-tri-*O*-acetyl-*β*-xylopyranosyl) azidoacetamide: Ph_3P, triphenyl phosphine; CH_2Cl_2, dichloromethane; NaN_3, sodium azide; DMF, *N*, *N*-dimethylformamide

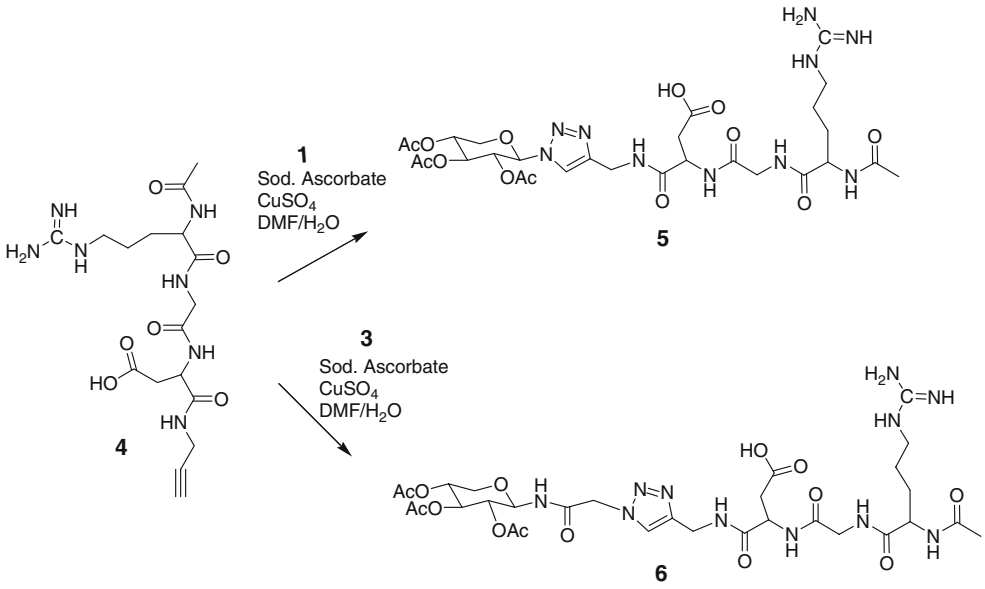

Scheme 2 Synthesis of linear RGD-conjugated xylosides using click chemistry: Sod. Ascorbate, sodium ascorbate; Cu_2SO_4, copper (II) sulfate; DMF, *N*, ***N***-dimethylformamide; H_2O, Deionized water

(m, 2H), 4.07–3.90 (m, 3H), 3.80–3.68 (m, 3H), 3.55–3.47 (m, 2H), 3.25–3.12 (m, 2H), 3.03 (t, J=13.58 Hz, 1H), 2.93 (dd, J=6.65 Hz, 13.28 Hz, 1H), 2.69–2.59 (m, 2H), 2.04 (s, 3H), 2.02 (s, 3H), 1.83 (s, 3H), 1.76–1.67 (m, 2H), 1.58–1.51 (m, 3H), 1.44–1.28 (m, 3H), 1.16–1.01 (m, 2H); MS (ESI): calcd for $C_{41}H_{57}N_{12}O_{15}$ $[M+H]^+$ 957.3988; found 957.2667.

Screening of RGD-xylosides in CHO cells, endothelial cells (BLMEC) and cancer cells (4T1): To determine whether the RGD-xylosides were able to prime GAG chains, the cells were treated with RGD-conjugated xylosides at various concentrations in the presence of $Na_2{}^{35}SO_4$. GAG chains were purified and analyzed as described below. $1x10^5$ cells were plated per well in complete growth medium in a 24 well plate. The cells were incubated at 37°C in a humidified incubator for 24 h to a confluence of about 50%. The cells were washed with sterile PBS and replaced with

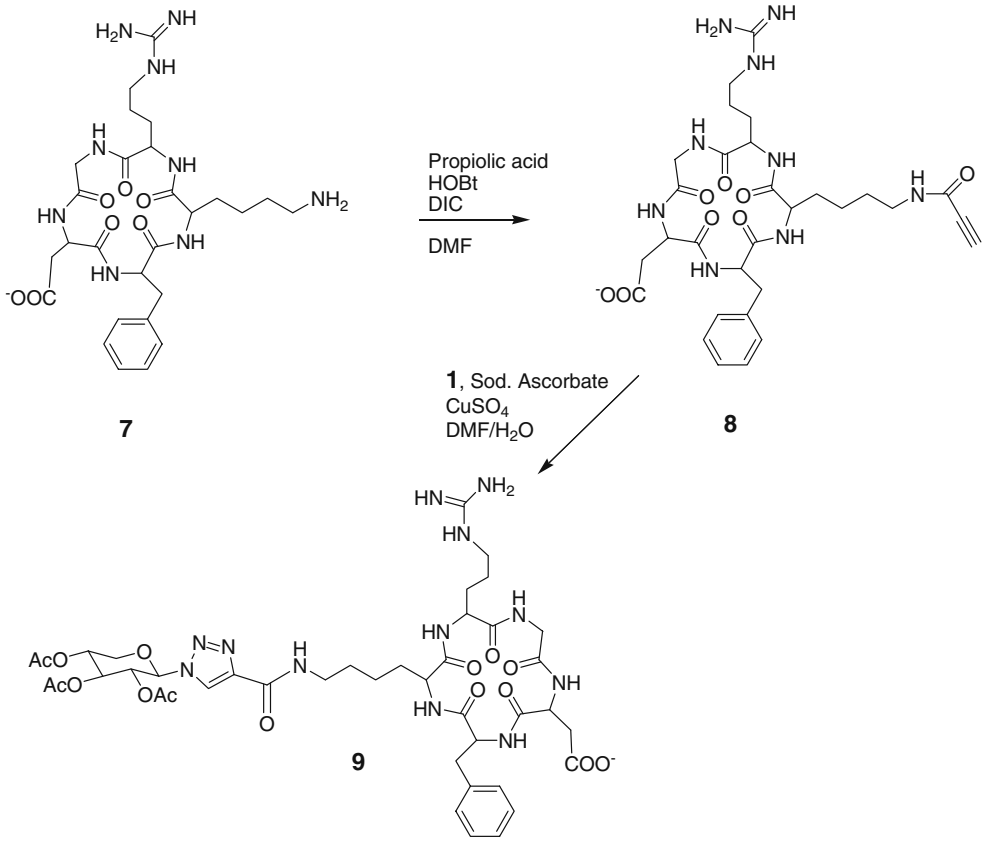

Scheme 3 Synthesis of cyclic RGD conjugated xyloside: HOBt, N-Hydroxybenzotriazole; DIC, 1,3-Disopropylcarbodimide; DMF, *N*, *N*-dimethylformamide; Sod. Ascorbate, sodium ascorbate; Cu_2SO_4, copper (II) sulfate; H_2O, Deionized water

495 μL Ham's/F12 containing 10% dialyzed FBS. A solution containing a specific primer at 100X the final concentration was prepared. 5 μL of appropriate 100X primer was added to various wells to yield the appropriate concentration and 50 μCi of $Na_2{}^{35}SO_4$ was also added to each well as tracer. The 24-well plates were incubated at 37°C in a humidified incubator (5% CO_2) for 24 h.

Purification and quantitation of GAG chains: The entire contents of the wells were transferred to a microcentrifuge tube and subjected to centrifugation at 16000 *x* g for 5 min. The supernatant was transferred to a fresh tube and 0.016% Triton X-100 (1.5 volumes) was added. The diluted supernatant was loaded on a 0.2 ml DEAE-sepharose column pre-equilibrated with 2 ml of wash buffer (20 mM NaOAc, 0.1 M NaCl and 0.01% Triton X-100, pH 6.0) and the column was washed with 6 ml of wash buffer. The bound HS/CS was eluted using 1.2 ml of elution buffer (20 mM NaOAc and 1 M NaCl, pH 6.0). The priming activities of xylosides 5, 6 & 9 were evaluated by quantitating the ^{35}S-radioactivity incorporated in to the purified HS/CS chains by liquid scintillation counter.

Sulfate density analysis of GAG chains: The purified GAG chains were analyzed by HPLC coupled to an inline radiomatic detector. Xyloside primed GAG chains of equal quantity were diluted five-fold with HPLC solvent A (10 mM KH_2PO_4, pH 6.0, 0.2% CHAPS) for anion exchange chromatography analysis. The sample was loaded on a HPLC-DEAE column and eluted from the column with a linear gradient of 0.2 M–1 M NaCl over 80 min at a flow rate of 1 ml/min. The radioactive GAG chains were detected by radiometric flo-one A505A detector. The HPLC effluent was mixed with Ultima-Flo AP scintillation cocktail in a 2:1 ratio and detected in the flow scintillation analyzer.

Chain length analysis of GAG chains primed by RGD-xylosides: The chain length of the GAG chains synthesized

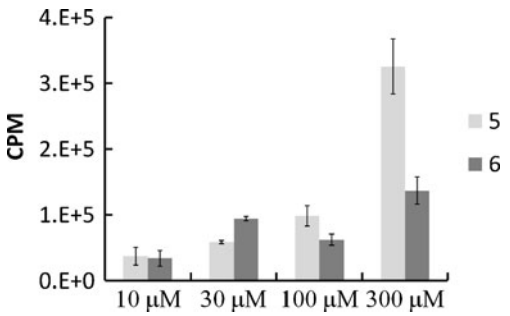

Fig. 1 Priming activity of two linear RGD-xylosides using pgs A-745 cell lines at various concentrations. CHO cells were treated with linear RGD xylosides 5 and 6 at 10, 30, 100 and 300 μM in the presence of $Na_2{}^{35}SO_4$ (50 μCi) as described in the experimental section. The GAG chains were purified by anion exchange chromatography and quantitated using liquid scintillation counter. The data shown is average of two independent experiments

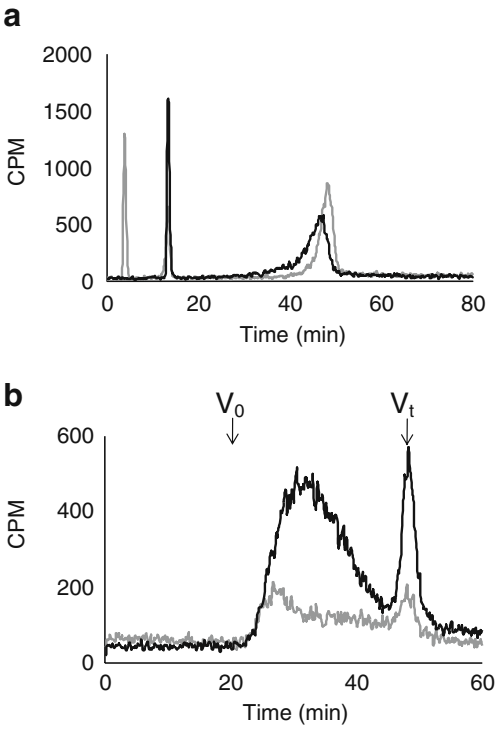

Fig. 2 **a** GAG chains primed by xyloside **5** in pgsA-745 cell lines were analyzed using anion exchange HPLC: The bound GAG chains were eluted with a linear gradient of 0.2 M to 1 M NaCl over 80 min at a flow rate of 1 ml/min. The elution profiles of GAG chains, primed at 100 μM (*grey*) and 300 μM (*black*), are shown. **b** The sizes of GAG chains primed by xyloside **5** in pgsA-745 cells were analyzed by size exclusion HPLC: the GAG chains, fractionated on two tandem 3000 $SW_L{}^X$ columns, were eluted with an isocratic gradient of phosphate buffer for 90 min at a flow rate of 0.5 ml/min as described in the experimental section. The elution profiles of the GAG chains primed at 100 μM (*grey trace*) and 300 μM (*black trace*) are shown. V_o and V_t represent void and total volume, respectively. These elution profiles are representative of two independent experiments

by various RGD-xyloside conjugates was determined by measuring migration time on a size exclusion column using a HPLC with inline radiodetector. The GAG chains were loaded on to two tandem G3000$SW_L{}^X$ columns (Tosoh, 7.8 mm×30 cm) and analyzed with the aid of an inline radiodetector using phosphate buffer (100 mM KH_2PO_4, 100 mM NaCl, pH 6) as eluant. The average molecular weight was determined by measuring the migration time of the GAG chains in comparison to those of polystyrene sulfonate standards performed under similar conditions.

Results and discussion

Synthesis of RGD-xylosides

In recent years, there has been great interest in assembling a number of biologically active carbohydrate conjugates using click chemistry because of its mild reaction con-

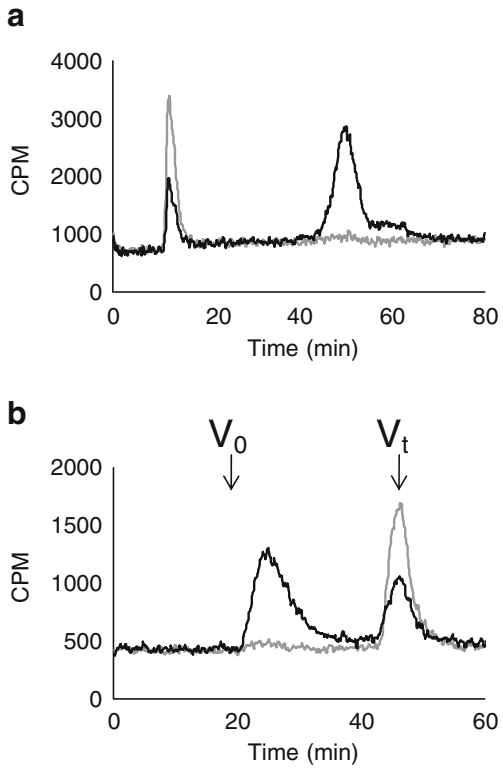

Fig. 3 **a** Anion exchange chromatography analysis of GAG chains produced by xyloside **9** in pgsA-745 cell lines: Purified GAG chains (grey trace for control cells and black trace for cells treated with 100 μM xyloside **9**) were analyzed using HPLC-DEAE anion exchange chromatography using a linear gradient of 0.2 M to 1 M NaCl as an eluant over 80 min at a flow rate of 1 ml/min. **b** Size exclusion profiles of GAG chains produced by xyloside 9 in pgsA-745 cell line: GAG chains were fractionated using two 3000 SW_L^X SEC columns that were connected in tandem using an isocratic gradient of phosphate buffer for 90 min at a flow rate of 0.5 ml/min as described in the experimental section (grey trace for control cells and black trace for cells treated with 100 μM xyloside **9**). V_o and V_t represent void and total volume, respectively. These elution profiles are representative of two independent experiments

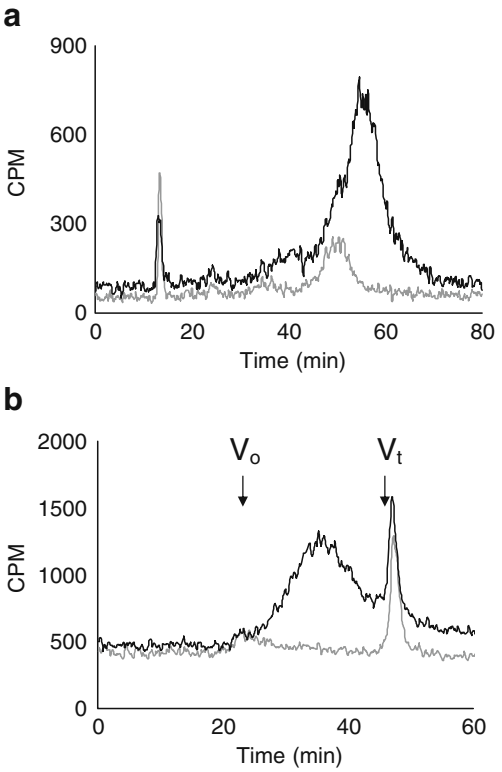

Fig. 4 **a** GAG chains, primed by xyloside **5** in endothelial cell line, were analyzed using anion exchange HPLC. The bound GAG chains were eluted with a linear gradient of 0.2 M to 1 M NaCl over 80 min at a flow rate of 1 ml/min. The radiodetector trace of the GAG chains isolated from control cells (*grey trace*) and cells treated with 100 μM xyloside (*black trace*) are shown. **b** GAG chains, primed by xyloside **5** in endothelial cell line, were analyzed using two SEC (3000 SW_L^X) that were connected in tandem and were eluted with an isocratic gradient of phosphate buffer for 90 min at a flow rate of 0.5 ml/min as described in the experimental section. The elution profile of the GAG chains, primed by xyloside **5** at 100 μM (black trace; control as grey trace), is shown. V_o and V_t represent void and total volume, respectively. These elution profiles are representative of two independent experiments

ditions, the generation of regioselective molecules with high efficiency in water and compatibility with most functional groups in biological systems [35–37]. This bioconjugation approach relies on the Cu(I)-catalyzed orthogonal reaction of azide containing xylosyl scaffold with terminal alkyne containing RGD motifs in the presence of other reactive functional groups. Furthermore, this approach offers two advantages: a) the 1, 2, 3-triazole ring generated during the click-chemistry is a metabolically stable linker between xylose residue and RGD peptide; b) the triazole ring can facilitate hydrogen-bonding interactions resulting in favorable and productive biological effects.

Xylosyl azide **1** was converted into **3** by first converting the azide group into the chloroacetamide followed by the replacement of the chloride group with an azide as shown in Scheme 1. These two xylosyl derivatives, **1** & **3**, contain reactive azide group for orthogonal coupling with RGD peptides containing terminal alkyne group in the subsequent steps. RGD peptides, **4** and **7**, were purchased from commercial sources. These RGD peptides were coupled with propargyl amine using well established coupling procedure. In a similar manner, cyclic RGD peptide **7** containing side chain amine group was reacted with propargylic acid under similar conditions to obtain propargylated cyclic RGD peptide **8** in high yield as shown in Scheme 3. After preparing appropriate orthogonally functionalized RGD peptides and xylosides, we turned to assembling RGD-conjugated xylosides, **5**, **6** and **9**, using click-chemistry as described in Schemes 2 and 3. The final products were purified on reverse phase C18 column using HPLC as described in the experimental section.

Priming activity of RGD-xylosides in CHO cells

The very first step in the biosynthesis of proteoglycans is the xylosylation of certain serine residues of the core protein [38]. Following xylosylation of the core protein, a tetrasaccharide linkage region, which serves as an acceptor site for elongation of GAG chains, is assembled [39–42]. It has been known for over three decades that GAG chains can also be assembled on xylosides without a core protein provided xylosides carry hydrophobic aglycone [20, 22]. We have synthesized various click-xylosides with hydrophobic moiety and demonstrated their ability to induce GAG chains in a cellular system [23]. A mutant Chinese hamster ovary [CHO] cell line, pgsA-745, is a convenient cellular system for determining the priming activity of exogenously supplied RGD-conjugated xylosides, because this cell line lacks active xylosyltransferase enzyme and therefore does not make endogenous GAG chains [43]. Thus, it is easier to determine whether RGD-conjugated xylosides induce GAG chains using this cell line. RGD-conjugated xylosides were screened in cell culture at various concentrations (10, 30, 100 and 300 μM). We found that the nature of linkage between xylose and RGD can affect the priming activity (Fig. 1). The results from priming activity analysis suggest that RGD-xyloside **5** is a better GAG primer than RGD-xyloside **6** at 100 μM and 300 μM. Therefore, the GAG chains primed by xyloside **5** were further analyzed for their sulfation pattern by DEAE-anion exchange HPLC column and for their molecular weights using size exclusion columns as outlined in the experimental section. It is interesting to note that the extent of sulfation of GAG chains primed by xylosides at 100 μM and 300 μM are nearly identical suggesting that these concentrations are optimal for GAG induction without challenging the Golgi machinery (Fig. 2). Nevertheless, Xyloside **5** primed nearly three times more GAG chains at 300 μM compare to 100 μM in CHO cells. The chain length of GAG chains primed by xyloside **5** in CHO cells was determined by measuring migration time of GAG chains in comparison to those of polystyrene sulfonate standards performed under similar conditions on size exclusion analyses and suggests that GAG chains, primed by xyloside **5** in CHO cells, have an average molecular weight of 45 KDa at 100 μM and 19 KDa at 300 μM concentration.

Cyclic RGD peptides are shown to bind more selectively than their linear motifs to $\alpha_v\beta_3$ integrin expressing activated endothelial cells and cancer cell lines [28, 44, 45]. Therefore, we synthesized xyloside conjugated to cyclic-RGD peptide motif **8**) using click-chemistry (Scheme 3). It is interesting to note that xyloside **9** primed GAG chains whose average molecular weight is higher than those primed by xyloside **5** in CHO cells. Xyloside **9** primed GAG chains migrated between 20–28 min in size exclusion column with average molecular weight of 67 KDa in comparison to those of polystyrene sulfonate standard (Fig. 3). GAG chains primed by xylosides **5** and **9** were digested with heparin lyases I, II and III to determine HS/CS composition. It is interesting to note that xyloside **5** primed about 50% HS chains, whereas Xylsoide **9** primed about 25% HS chains. Xyloside **6**, on the other hand, primed about 80% HS chains even though this scaffold has lower priming activity than Xyloside **5**.

Priming activity of xylosides in endothelial cells (BLMVEC) and cancer cell line (4T1)

$\alpha_v\beta_3$ integrin receptors are elevated in activated endothelial cells, angiogenic cardiomyocytes and highly vascularized

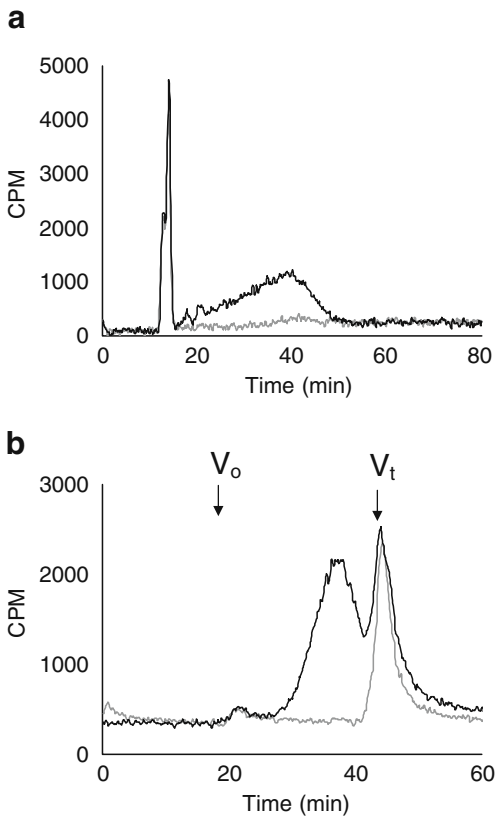

Fig. 5 **a** GAG chains primed by xyloside **5** in cancer cell line were analyzed using anion exchange HPLC. The bound GAG chains were eluted with a linear salt gradient for 80 min as described in the experimental section. The radiodetector trace of the eluted GAG chains from control cells (*grey trace*) and cells treated with 100 μM xyloside (*black trace*) are shown. **b** GAG chains primed by xyloside **5** in 4T1 cell line were analyzed using SEC column as described in the experimental section, were eluted with an isocratic gradient of phosphate buffer for 90 min at a flow rate of 0.5 ml/min. The radiodetector traces of the eluted GAG chains, primed by xyloside **5** at 100 μM (*black trace*) and control cells (*grey trace*), are shown. These elution profiles shown here are representative of two independent experiments

cancer cells, and therefore, RGD-conjugated xylosides are expected to be up taken by these cells. For these reasons, we chose to determine the priming activity of RGD-conjugated xylosides in endothelial cells (BLMVEC) and mouse breast cancer cell line (4T1). The priming activity of RGD xylosides in endothelial cells and cancer cells are determined as described earlier for CHO cells. The xyloside **5** did prime on both endothelial cells and cancer cells (Figs. 4 and 5). Xyloside **5** was able to induce GAG chains by 6-fold in endothelial cells and 3-fold in cancer cell line. Molecular weight of GAG chains primed by xyloside **5** was found to be~10 KDa in the endothelial cell and cancer cell line. It was disappointing to note that cyclic-RGD conjugated xyloside **9** was unable to prime GAG chains in either the endothelial cells or cancer cell line. It is possible that the cyclic-RGD motif may prevent the selective transport of xyloside to the Golgi machinery, where they prime GAG chains. Alternatively, cyclic motif may sterically interfere with biosynthetic enzymes preventing the priming of GAG chains by xyloside **9**. For these reasons, we plan to make a library of cyclic-RGD motifs with variable distance between the xylose and the peptide with an aim to discover new scaffolds that prime GAG chains.

In summary, we have successfully synthesized RGD-conjugated xylosides that target cells displaying the $\alpha_v\beta_3$ integrin using click chemistry. These RGD-conjugated homing xylosides are able to prime GAG chains in various cellular systems indicating their likely applications in tackling MI, thrombosis and cancer associated vascular complications, where GAG chains are known to modulate various pathological processes. Future studies will focus on the synthesis of additional homing xylosides and evaluation of their pharmacokinetics and pharmacodynamics in various animal models.

Acknowledgment This work was supported by NIH (GM075168) and Human Frontier Science Program grants to BK.

References

1. Cummings, R.D.: The repertoire of glycan determinants in the human glycome. Mol. Biosyst. **5**, 1087–1104 (2009)
2. Damus, P.S., Hicks, M., Rosenberg, R.D.: Anticoagulant action of heparin. Nature. **246**, 355–357 (1973)
3. Hopwood, J., Hook, M., Linker, A., Lindahl, U.: Anticoagulant activity of heparin: isolation of antithrombin-binding sites. FEBS Lett. **69**, 51–54 (1976)
4. Kuberan, B., Lech, M.Z., Beeler, D.L., Wu, Z.L., Rosenberg, R. D.: Enzymatic synthesis of antithrombin III-binding heparan sulfate pentasaccharide. Nat. Biotechnol. **21**, 1343–1346 (2003)
5. Sasisekharan, R., Shriver, Z., Venkataraman, G., Narayanasami, U.: Roles of heparan-sulphate glycosaminoglycans in cancer. Nat. Rev. Cancer. **2**, 521–528 (2002)
6. Raman, K., Kuberan, B.: Chemical tumor biology of heparan sulfate proteoglycans. Curr. Chem. Biol. **4**, 20–31 (2010)
7. Purushothaman, A., Chen, L., Yang, Y., Sanderson, R.D.: Heparanase stimulation of protease expression implicates it as a master regulator of the aggressive tumor phenotype in myeloma. J. Biol. Chem. **283**, 32628–32636 (2008)
8. Fux, L., Ilan, N., Sanderson, R.D., Vlodavsky, I.: Heparanase: busy at the cell surface. Trends Biochem. Sci. **34**, 511–519 (2009)
9. Vlodavsky, I., Ilan, N., Nadir, Y., Brenner, B., Katz, B.Z., Naggi, A., Torri, G., Casu, B., Sasisekharan, R.: Heparanase, heparin and the coagulation system in cancer progression. Thromb. Res. **120** (Suppl. 2), S112–120 (2007)
10. Yang, J., Price, M.A., Neudauer, C.L., Wilson, C., Ferrone, S., Xia, H., Iida, J., Simpson, M.A., McCarthy, J.B.: Melanoma chondroitin sulfate proteoglycan enhances FAK and ERK activation by distinct mechanisms. J. Cell Biol. **165**, 881–891 (2004)
11. Yip, G.W., Smollich, M., Gotte, M.: Therapeutic value of glycosaminoglycans in cancer. Mol. Cancer Ther. **5**, 2139–2148 (2006)
12. Varki, N.M., Varki, A.: Heparin inhibition of selectin-mediated interactions during the hematogenous phase of carcinoma metastasis: rationale for clinical studies in humans. Semin. Thromb. Hemost. **28**, 53–66 (2002)
13. Borsig, L., Wong, R., Feramisco, J., Nadeau, D.R., Varki, N.M., Varki, A.: Heparin and cancer revisited: mechanistic connections involving platelets, P-selectin, carcinoma mucins, and tumor metastasis. Proc. Natl. Acad. Sci. U. S. A. **98**, 3352–3357 (2001)
14. Kishimoto, T.K., Viswanathan, K., Ganguly, T., Elankumaran, S., Smith, S., Pelzer, K., Lansing, J.C., Sriranganathan, N., Zhao, G., Galcheva-Gargova, Z., Al-Hakim, A., Bailey, G.S., Fraser, B., Roy, S., Rogers-Cotrone, T., Buhse, L., Whary, M., Fox, J., Nasr, M., Dal Pan, G.J., Shriver, Z., Langer, R.S., Venkataraman, G., Austen, K.F., Woodcock, J., Sasisekharan, R.: Contaminated heparin associated with adverse clinical events and activation of the contact system. N. Engl. J. Med. **358**, 2457–2467 (2008)
15. Blossom, D.B., Kallen, A.J., Patel, P.R., Elward, A., Robinson, L., Gao, G., Langer, R., Perkins, K.M., Jaeger, J.L., Kurkjian, K.M., Jones, M., Schillie, S.F., Shehab, N., Ketterer, D., Venkataraman, G., Kishimoto, T.K., Shriver, Z., McMahon, A.W., Austen, K.F., Kozlowski, S., Srinivasan, A., Turabelidze, G., Gould, C.V., Arduino, M.J., Sasisekharan, R.: Outbreak of adverse reactions associated with contaminated heparin. N. Engl. J. Med. **359**, 2674–2684 (2008)
16. Gibson, K.D., Segen, B.J., Audhya, T.K.: The effect of beta-D-xylosides on chondroitin sulphate biosynthesis in embryonic chicken cartilage in the absence of protein synthesis inhibitors. Biochem. J. **162**, 217–233 (1977)
17. Schwartz, N.B., Ho, P.L., Dorfman, A.: Effect of beta-xylosides on synthesis of cartilage-specific proteoglycan in chondrocyte cultures. Biochem. Biophys. Res. Commun. **71**, 851–856 (1976)
18. Robinson, H.C., Brett, M.J., Tralaggan, P.J., Lowther, D.A., Okayama, M.: The effect of D-xylose, beta-D-xylosides and beta-D-galactosides on chondroitin sulphate biosynthesis in embryonic chicken cartilage. Biochem. J. **148**, 25–34 (1975)
19. Galligani, L., Hopwood, J., Schwartz, N.B., Dorfman, A.: Stimulation of synthesis of free chondroitin sulfate chains by beta-D-xylosides in cultured cells. J. Biol. Chem. **250**, 5400–5406 (1975)
20. Schwartz, N.B., Galligani, L., Ho, P.L., Dorfman, A.: Stimulation of synthesis of free chondroitin sulfate chains by beta-D-xylosides in cultured cells. Proc. Natl. Acad. Sci. U. S. A. **71**, 4047–4051 (1974)
21. Abrahamsson, C.O., Ellervik, U., Eriksson-Bajtner, J., Jacobsson, M., Mani, K.: Xylosylated naphthoic acid-amino acid conjugates for investigation of glycosaminoglycan priming. Carbohydr. Res. **343**, 1473–1477 (2008)
22. Okayama, M., Kimata, K., Suzuki, S.: The influence of p-nitrophenyl beta-d-xyloside on the synthesis of proteochondroitin sulfate by slices of embryonic chick cartilage. J. Biochem. **74**, 1069–1073 (1973)

23. Kuberan, B., Ethirajan, M., Victor, X.V., Tran, V., Nguyen, K., Do, A.: "Click" xylosides initiate glycosaminoglycan biosynthesis in a mammalian cell line. Chembiochem. **9**, 198–200 (2008)
24. Fritz, T.A., Lugemwa, F.N., Sarkar, A.K., Esko, J.D.: Biosynthesis of heparan sulfate on beta-D-xylosides depends on aglycone structure. J. Biol. Chem. **269**, 300–307 (1994)
25. Victor, X.V., Nguyen, T.K., Ethirajan, M., Tran, V.M., Nguyen, K. V., Kuberan, B.: Investigating the elusive mechanism of glycosaminoglycan biosynthesis. J. Biol. Chem. **284**, 25842–25853 (2009)
26. DeNardo, S.J., Burke, P.A., Leigh, B.R., O'Donnell, R.T., Miers, L.A., Kroger, L.A., Goodman, S.L., Matzku, S., Jonczyk, A., Lamborn, K.R., DeNardo, G.L.: Neovascular targeting with cyclic RGD peptide (cRGDf-ACHA) to enhance delivery of radioimmunotherapy. Cancer Biother. Radiopharm. **15**, 71–79 (2000)
27. Meyer, A., Auernheimer, J., Modlinger, A., Kessler, H.: Targeting RGD recognizing integrins: drug development, biomaterial research, tumor imaging and targeting. Curr. Pharm. Des. **12**, 2723–2747 (2006)
28. Park, K., Kim, Y.S., Lee, G.Y., Park, R.W., Kim, I.S., Kim, S.Y., Byun, Y.: Tumor endothelial cell targeted cyclic RGD-modified heparin derivative: inhibition of angiogenesis and tumor growth. Pharm. Res. **25**, 2786–2798 (2008)
29. Carlson, C.B., Mowery, P., Owen, R.M., Dykhuizen, E.C., Kiessling, L.L.: Selective tumor cell targeting using low-affinity, multivalent interactions. ACS Chem. Biol. **2**, 119–127 (2007)
30. Owen, R.M., Carlson, C.B., Xu, J., Mowery, P., Fasella, E., Kiessling, L.L.: Bifunctional ligands that target cells displaying the alpha v beta3 integrin. Chembiochem. **8**, 68–82 (2007)
31. Wang, W., Borchardt, R.T., Wang, B.: Orally active peptidomimetic RGD analogs that are glycoprotein IIb/IIIa antagonists. Curr. Med. Chem. **7**, 437–453 (2000)
32. Gyorgydeak, Z., Szilagyi, L., Paulsen, H.: Synthesis, structure, and reactions of glycosyl azide. J. Carbohydr. Chem. **12**, 139–163 (1993)
33. Inazu, T., Kobayashi, K.: A new method for the synthesis of N^{α}-Fmoc-N^{β}-glycosylated-L-asparagine derivatives. Synlett. 869–870 (1993)
34. Aich, U., Loganathan, D.: Synthesis of N-(beta-glycopyranosyl) azidoacetamides. J. Carbohydr. Chem. **24**, 1–12 (2005)
35. Tornoe, C.W., Christensen, C., Meldal, M.: Peptidotriazoles on solid phase: [1, 2, 3]-triazoles by regiospecific copper(i)-catalyzed 1, 3-dipolar cycloadditions of terminal alkynes to azides. J. Org. Chem. **67**, 3057–3064 (2002)
36. Meldal, M., Tornoe, C.W.: Cu-catalyzed azide-alkyne cycloaddition. Chem. Rev. **108**, 2952–3015 (2008)
37. Bertozzi, C.R., Kiessling, L.L.: Chemical glycobiology. Science. **291**, 2357–2364 (2001)
38. Lindahl, U., Roden, L.: The role of galactose and xylose in the linkage of heparin to protein. J. Biol. Chem. **240**, 2821–2826 (1965)
39. Sugahara, K.: The carbohydrate-protein linkage region of proteoglycans and glycosaminoglycan biosynthesis. Seikagaku. **61**, 496–500 (1989)
40. Kitagawa, H., Oyama, M., Masayama, K., Yamaguchi, Y., Sugahara, K.: Structural variations in the glycosaminoglycan-protein linkage region of recombinant decorin expressed in Chinese hamster ovary cells. Glycobiology. **7**, 1175–1180 (1997)
41. Kitagawa, H., Tone, Y., Tamura, J., Neumann, K.W., Ogawa, T., Oka, S., Kawasaki, T., Sugahara, K.: Molecular cloning and expression of glucuronyltransferase I involved in the biosynthesis of the glycosaminoglycan-protein linkage region of proteoglycans. J. Biol. Chem. **273**, 6615–6618 (1998)
42. Gulberti, S., Lattard, V., Fondeur, M., Jacquinet, J.C., Mulliert, G., Netter, P., Magdalou, J., Ouzzine, M., Fournel-Gigleux, S.: Phosphorylation and sulfation of oligosaccharide substrates critically influence the activity of human beta1, 4-galactosyltransferase 7 (GalT-I) and beta1, 3-glucuronosyltransferase I (GlcAT-I) involved in the biosynthesis of the glycosaminoglycan-protein linkage region of proteoglycans. J. Biol. Chem. **280**, 1417–1425 (2005)
43. Esko, J.D., Stewart, T.E., Taylor, W.H.: Animal cell mutants defective in glycosaminoglycan biosynthesis. Proc. Natl. Acad. Sci. U. S. A. **82**, 3197–3201 (1985)
44. Pfaff, M., Tangemann, K., Muller, B., Gurrath, M., Muller, G., Kessler, H., Timpl, R., Engel, J.: Selective recognition of cyclic RGD peptides of NMR defined conformation by alpha IIb beta 3, alpha V beta 3, and alpha 5 beta 1 integrins. J. Biol. Chem. **269**, 20233–20238 (1994)
45. Kaufmann, D., Fiedler, A., Junger, A., Auernheimer, J., Kessler, H., Weberskirch, R.: Chemical conjugation of linear and cyclic RGD moieties to a recombinant elastin-mimetic polypeptide—a versatile approach towards bioactive protein hydrogels. Macromol. Biosci. **8**, 577–588 (2008)